




Centrum voor Wiskunde en Informatica

View metadata, citation and similar papers at core.ac.uk

brought to you by  CORE

provided by CWI's Institutions

REPORTRAPPORT

MAS

Modelling, Analysis and Simulation



Modelling, Analysis and Simulation

Runge-Kutta methods and viscous wave equations

J.G. Verwer

REPORT MAS-E0803 MARCH 2008

Centrum voor Wiskunde en Informatica (CWI) is the national research institute for Mathematics and Computer Science. It is sponsored by the Netherlands Organisation for Scientific Research (NWO). CWI is a founding member of ERCIM, the European Research Consortium for Informatics and Mathematics.

CWI's research has a theme-oriented structure and is grouped into four clusters. Listed below are the names of the clusters and in parentheses their acronyms.

Probability, Networks and Algorithms (PNA)

Software Engineering (SEN)

Modelling, Analysis and Simulation (MAS)

Information Systems (INS)

Copyright © 2008, Stichting Centrum voor Wiskunde en Informatica
P.O. Box 94079, 1090 GB Amsterdam (NL)
Kruislaan 413, 1098 SJ Amsterdam (NL)
Telephone +31 20 592 9333
Telefax +31 20 592 4199

ISSN 1386-3703

Runge-Kutta methods and viscous wave equations

ABSTRACT

We study the numerical time integration of a class of viscous wave equations by means of Runge-Kutta methods. The viscous wave equation is an extension of the standard second-order wave equation including advection-diffusion terms differentiated in time. The viscous wave equation can be very stiff so that for time integration traditional explicit methods are no longer efficient. A-stable Runge-Kutta methods are then very good candidates for time integration, in particular diagonally implicit ones.

2000 Mathematics Subject Classification: 65L05, 65L06, 65L20, 65M12, 65M20

1998 ACM Computing Classification System: G.1.7, G.1.8

Keywords and Phrases: Viscous wave equations, numerical integration, Runge-Kutta methods

Runge-Kutta Methods and Viscous Wave Equations

J.G. Verwer

Center for Mathematics and Computer Science

P.O. Box 94079, 1090 GB Amsterdam, The Netherlands

Jan.Verwer@cwi.nl

March 3, 2008

Abstract

We study the numerical time integration of a class of viscous wave equations by means of Runge-Kutta methods. The viscous wave equation is an extension of the standard second-order wave equation including advection-diffusion terms differentiated in time. The viscous wave equation can be very stiff so that for time integration traditional explicit methods are no longer efficient. A -stable Runge-Kutta methods are then very good candidates for time integration, in particular diagonally implicit ones.

2000 Mathematics Subject Classification: Primary: 65L05, 65L06, 65L20, 65M12, 65M20.

1998 ACM Computing Classification System: G.1.7, G.1.8.

Keywords and Phrases: Viscous wave equations, numerical time integration, Runge-Kutta methods.

Note: Work carried out within theme MAS1.

1 Introduction

In this paper we discuss the application of Runge-Kutta methods for the numerical time integration of viscous wave equations of the form

$$U_{tt} = (\mathcal{L}_1 U)_t + \mathcal{L}_2 U, \quad (1.1)$$

where \mathcal{L}_1 and \mathcal{L}_2 are the linear spatial operators

$$\mathcal{L}_1 U = \gamma_1 U - \nabla \cdot (\underline{a} U) + \nabla \cdot (D_1 \nabla U), \quad \mathcal{L}_2 U = \gamma_2 U + \nabla \cdot (D_2 \nabla U) + S. \quad (1.2)$$

Here, γ_1 and γ_2 are non-positive scalars, \underline{a} is a velocity field in \mathbb{R}^d , D_1 and D_2 are symmetric nonnegative diffusion tensors in $\mathbb{R}^{d \times d}$ and S is a source term. The scalar γ_2 and tensor D_2 are not allowed to vanish simultaneously and except S all coefficients are supposed to depend on the spatial variable only. The equation is to be provided with initial values for U and U_t at time $t = 0$ and properly chosen boundary conditions on the boundary of a bounded space domain in \mathbb{R}^d . As a special case we have the non-viscous (acoustic) wave equation

$$U_{tt} = \nabla \cdot (D_2 \nabla U) + S. \quad (1.3)$$

For our numerical treatment we write (1.1) in the first-order system form

$$\begin{aligned} U_t &= \mathcal{L}_1 U + V, \\ V_t &= \mathcal{L}_2 U. \end{aligned} \quad (1.4)$$

The linear equation (1.1) and likewise (1.4) is called a viscous or damped wave equation due to the terms $(\mathcal{L}_1 U)_t$ and $\gamma_2 U$. For zero velocity \underline{a} this particular viscous wave equation has been

studied extensively in [9, 16] in connection with splitting methods. The equation is numerically interesting as it is a mixture of the second-order in time wave equation and the first-order in time advection-diffusion equation. If γ_1, γ_2 and D_1 simultaneously vanish while $\underline{u} \neq 0$ the equation has no viscous terms left. For convenience of discussion also in this case we will use the name viscous wave equation. Applications are found in acoustic wave propagation and microscale heat transfer [9, 16]. In [21] we have considered explicit time integration of (1.1) for a zero velocity \underline{u} by means of a tuned stabilized, explicit Runge-Kutta method. In the current paper we discuss general Runge-Kutta methods for time integration including explicit and implicit methods.

The contents of the paper is as follows. Section 2 is devoted to a general semi-discrete approximation of (1.1). Herewith we follow the method of lines approach. In this section we discuss a number of stability properties of the semi-discrete approximation. In Section 3 we introduce the Runge-Kutta method and discuss stability properties including algebraic stability and A -stability and the notion of stability region. In this section we also pay attention to order reduction caused by stiff source terms emanating from time-dependent boundary conditions. An immediate consequence of adding viscous terms is stiffness. The final Section 4 is therefore devoted to further numerical illustrations with a highly stiff test example.

2 The semi-discrete problem

We follow the method of lines approach and thus suppose an appropriate spatial discretization of (1.4) with its boundary conditions in a domain in \mathbb{R}^d towards an initial value problem for a partitioned system of continuous-time ordinary differential equations

$$\begin{aligned} u' &= F_1(t, u) + v, & t > 0, & \quad u(0) = u_0, \\ v' &= F_2(t, u), & t > 0, & \quad v(0) = v_0. \end{aligned} \tag{2.1}$$

The dependent variables u and v thus are vector (grid) functions approximating U and V and the vector functions $F_1(t, u)$ and $F_2(t, u)$ are associated to $\mathcal{L}_1 U$ and $\mathcal{L}_2 U$, respectively.¹⁾ For simplicity of presentation we do not explicitly include finite element mass matrices in our notation because Runge-Kutta formulas are easily adjusted to cater for mass matrices. We suppose $u, v \in \mathbb{R}^m$ whereby dimension $m = m(h)$ is variable as it depends on the spatial grid size here represented by h . Assuming the partitioning $w = (u, v)$ and $F = (F_1, F_2)$ we will also use the generic ODE system notation

$$w' = F(t, w), \quad t > 0, \quad w(0) = w_0. \tag{2.2}$$

Due to linearity, (2.1) and (2.2) take the form

$$\begin{aligned} u' &= A_1 u + v + s_1(t), \\ v' &= A_2 u + s_2(t), \end{aligned} \tag{2.3}$$

and

$$w' = Aw + s(t), \quad A = \begin{pmatrix} A_1 & I \\ A_2 & 0 \end{pmatrix}, \quad s(t) = \begin{pmatrix} s_1(t) \\ s_2(t) \end{pmatrix}, \tag{2.4}$$

where A_1 and A_2 are constant matrices in $\mathbb{R}^{m \times m}$ associated to \mathcal{L}_1 and \mathcal{L}_2 , respectively, and $s_1(t)$ and $s_2(t)$ may contain contributions from sources and boundaries. This linear formulation covers all possible semi-discrete approximations to the linear problem (1.4) and its boundary conditions. Observe that (2.3) and (2.4) are just first-order representations of the second-order linear oscillator-type system

$$u'' - A_1 u' - A_2 u = s(t), \quad s(t) = s_1'(t) + s_2(t). \tag{2.5}$$

¹⁾ For formulating the Runge-Kutta formulas we prefer to use this nonlinear notation.

2.1 Stability results based on inner product norms

According to the method of lines approach we take the linear ODE systems (2.3) and (2.4) as our starting point for the numerical analysis. Assuming zero source terms, for that purpose we will first give analytical stability results for which we introduce Ansatz 2.1-2.2. The stability concept we are after in the current section is $w(t)$ bounded for all $t \geq 0$ in an appropriate inner product norm $\|\cdot\|$ determined by the Ansatz. The use of inner product norms enables us to prove the same stability results for almost all known implicit Runge-Kutta methods.

Ansatz 2.1 *With respect to an inner product $\langle \cdot, \cdot \rangle$ in \mathbb{R}^m the matrices A_1 and A_2 satisfy*

$$\langle A_1 u, A_2 u \rangle \geq -\omega_1 \|u\|^2 \quad \text{and} \quad \langle A_2 u, \tilde{u} \rangle = \langle u, A_2 \tilde{u} \rangle, \quad \langle A_2 u, u \rangle \leq 0 \quad (2.6)$$

for any $u, \tilde{u} \in \mathbb{R}^m$ where ω_1 is a real constant independent of m and u, \tilde{u} .²⁾ \diamond

Hence we assume A_2 symmetric and non-positive definite which in view of the conditions imposed on γ_2 and D_2 is a natural property. For A_1 we impose the first condition whereby independence of ω_1 on m is assumed so that this condition holds uniformly with respect to the underlying spatial grids. Denote $A_2^- = -A_2$ and consider in \mathbb{R}^{2m} the inner product

$$\langle w, \tilde{w} \rangle_A = \langle u, A_2^- \tilde{u} \rangle + \langle v, \tilde{v} \rangle \quad (2.7)$$

with the associated squared norm

$$\|w\|_A^2 = \langle u, A_2^- u \rangle + \|v\|^2. \quad (2.8)$$

Omitting the source terms and using

$$\langle Aw, w \rangle_A = \langle A_1 u + v, A_2^- u \rangle + \langle A_2 u, v \rangle = \langle A_1 u, A_2^- u \rangle, \quad (2.9)$$

Ansatz 2.1 then leads to the following solution norm inequality for (2.3),

$$\frac{1}{2} \frac{d}{dt} \|w\|_A^2 = \langle Aw, w \rangle_A = \langle A_1 u, A_2^- u \rangle \leq \omega_1 \|u\|^2. \quad (2.10)$$

Hence if $\omega_1 \leq 0$ we have stability in time for all $t \geq 0$, that is, $\|w(t)\|$ bounded for all $t \geq 0$. If $\omega_1 > 0$ this result merely implies a bounded solution over a finite time interval, but with a growth factor independent of the spatial grid size. Further, if $\langle A_1 u, A_2 u \rangle = 0$ we have got the conservation property

$$\frac{d}{dt} \|w\|_A^2 = \langle Aw, w \rangle_A = 0. \quad (2.11)$$

This holds trivially for a zero A_1 matrix and for a skew-symmetric matrix A_1 that commutes with A_2 . Needless to say that these properties are meaningful with respect to component u only if the contribution $\langle u, A_2^- u \rangle$ within norm (2.8) is strictly positive.

Ansatz 2.2 *With respect to an inner product $\langle \cdot, \cdot \rangle$ in \mathbb{R}^m the matrices A_1 and A_2 satisfy*

$$\langle A_1 u, u \rangle \leq \omega_1 \|u\|^2 \quad \text{and} \quad \langle A_2 u, \tilde{u} \rangle = \langle u, A_2 \tilde{u} \rangle, \quad \langle A_2 u, u \rangle < 0 \quad (2.12)$$

for any $u, \tilde{u} \in \mathbb{R}^m$ where ω_1 is a real constant independent of m and u, \tilde{u} . \diamond

Now we take A_2 symmetric negative definite so that we may consider in \mathbb{R}^{2m} the inner product

$$\langle w, \tilde{w} \rangle_{A^{-1}} = \langle u, \tilde{u} \rangle + \langle v, (A_2^-)^{-1} \tilde{v} \rangle \quad (2.13)$$

²⁾ Here and in the following the symbol u thus denotes a solution of (2.3) as well as an arbitrary vector in \mathbb{R}^m . The symbols v and w will be used similarly. The specific meaning will always be clear from the context.

with the associated squared norm

$$\|w\|_{A^{-1}}^2 = \|u\|^2 + \langle v, (A_2^-)^{-1}v \rangle. \quad (2.14)$$

In this norm the following inequality readily follows,

$$\frac{1}{2} \frac{d}{dt} \|w\|_{A^{-1}}^2 = \langle Aw, w \rangle_{A^{-1}} = \langle A_1 u, u \rangle \leq \omega_1 \|u\|^2. \quad (2.15)$$

Taking into account that \mathcal{L}_1 in (1.1) is an advection-diffusion operator, the assumption on A_1 will cover a wide problem class. We now have stability for all $t \geq 0$ if $\omega_1 \leq 0$. If $\omega_1 > 0$ we can guarantee a bounded solution over finite time intervals only but with growth factors independent of spatial grid sizes. Trivially, we have again conservation if A_1 is skew-symmetric while commutation with A_2 is not needed here.

Remark 2.3 The relation between conservation and skew-symmetry of matrix A_1 can also be shown as follows. If A_2 is symmetric negative definite A is similar to

$$\tilde{A} = \begin{pmatrix} A_1 & L \\ -L^T & 0 \end{pmatrix} = \begin{pmatrix} I & 0 \\ 0 & L \end{pmatrix}^{-1} \begin{pmatrix} A_1 & I \\ A_2 & 0 \end{pmatrix} \begin{pmatrix} I & 0 \\ 0 & L \end{pmatrix}, \quad (2.16)$$

where L is the lower triangular matrix defined by the Cholesky decomposition $A_2 = -LL^T$ [10]. Obviously, \tilde{A} is skew-symmetric if and only if A_1 is skew-symmetric, in which case the eigenvalue spectrum of matrix A is purely imaginary which is necessary for conservation. A skew-symmetric matrix A_1 would be obtained if we define $\mathcal{L}_1 U$ in (1.1) by an advection term $-\nabla \cdot (\underline{a}U)$ for some constant velocity field \underline{a} and then spatially discretize $\mathcal{L}_1 U$ symmetrically. \diamond

2.2 Stability results based on eigenvalues

Analytical stability results based on inner product norms as derived above are generally not applicable to explicit Runge-Kutta methods. In the current section we therefore proceed with eigenvalue analysis which will enable us to use the celebrated numerical concept of stability region for explicit methods. Considering system (2.4) with a zero source term, eigenvalue analysis starts from its exponential matrix solution expression $w(t) = e^{At}w(0)$. Two cases are distinguished covered by Ansatz (2.4) and (2.5) below.

Ansatz 2.4 Matrix A_1 is similar to a diagonal eigenvalue matrix with eigenvalues λ_1 satisfying $\text{Re}(\lambda_1) \leq 0$. Matrix A_2 is similar to a diagonal eigenvalue matrix with real non-positive eigenvalues λ_2 . Further, A_1 and A_2 share their set of eigenvectors which in addition does have a condition number independent of m . \diamond

Note that we now assume that A_1 commutes with A_2 . Let X denote the shared eigenvector matrix such that $A_k = X\Lambda_k X^{-1}$. Then

$$A = \hat{X}\hat{A}\hat{X}^{-1}, \quad \hat{X} = \begin{pmatrix} X & 0 \\ 0 & X \end{pmatrix}, \quad \hat{A} = \begin{pmatrix} \Lambda_1 & I \\ \Lambda_2 & 0 \end{pmatrix}, \quad \hat{w} = \hat{X}^{-1}w, \quad (2.17)$$

and we see that the temporal stability is determined by stability of the transformed system

$$\hat{w}' = \hat{A}\hat{w}, \quad \hat{A} = \begin{pmatrix} \Lambda_1 & I \\ \Lambda_2 & 0 \end{pmatrix}, \quad (2.18)$$

that is, in an appropriate norm,

$$\|w(t)\| \leq \text{cond}(\hat{X}) \|w(0)\| \|e^{\hat{A}t}\|, \quad t \geq 0. \quad (2.19)$$

So our task is to examine stability of (2.18) whereby the conditioning assumption serves to eliminate space grid dependence. The blocks of matrix \hat{A} are diagonal. Keeping the same notation for convenience, this means that stability of (2.18) is determined by the stability of all m 2×2 -systems

$$\hat{w}' = \hat{A}\hat{w} \quad \text{defined by} \quad \begin{pmatrix} \hat{u}' \\ \hat{v}' \end{pmatrix} = \begin{pmatrix} \lambda_1 & 1 \\ \lambda_2 & 0 \end{pmatrix} \begin{pmatrix} \hat{u} \\ \hat{v} \end{pmatrix}, \quad (2.20)$$

where \hat{u}, \hat{v} now denote components of $X^{-1}u, X^{-1}v$ and λ_1 and λ_2 belong to a shared eigenvector.

Having a shared set of eigenvectors obviously puts a restriction on A_1 and A_2 . It holds for example for Toeplitz matrices which arise with constant (in space) coefficients and periodic boundary conditions for (1.1). In this case A_1 and A_2 are normal and X is orthogonal giving an L_2 -condition number equal to one. Because \mathcal{L}_1 is an advection-diffusion operator it is natural to consider eigenvalues λ_1 with imaginary parts.

We proceed with the 2×2 -system (2.20). Assuming $\lambda_2 < 0$, stability then follows trivially from the similarity transformation

$$\hat{A} = \begin{pmatrix} \lambda_1 & 1 \\ \lambda_2 & 0 \end{pmatrix} = \begin{pmatrix} \frac{\lambda_+}{\lambda_2} & \frac{\lambda_-}{\lambda_2} \\ 1 & 1 \end{pmatrix} \begin{pmatrix} \lambda_+ & 0 \\ 0 & \lambda_- \end{pmatrix} \begin{pmatrix} \frac{\lambda_+}{\lambda_2} & \frac{\lambda_-}{\lambda_2} \\ 1 & 1 \end{pmatrix}^{-1} \quad (2.21)$$

resulting in the eigenvalue pairs

$$\lambda_{\pm} = \frac{1}{2} \left(\lambda_1 \pm \sqrt{\lambda_1^2 + 4\lambda_2} \right) \quad \text{satisfying} \quad \text{Re}(\lambda_{\pm}) \leq 0. \quad (2.22)$$

For $\lambda_2 = 0$ the similarity transformation does not exist. In this case we conclude stability directly from the exact solution

$$\hat{u}(t) = e^{\lambda_1 t} \hat{u}(0) + \frac{e^{\lambda_1 t} - 1}{\lambda_1} \hat{v}(0), \quad \hat{v}(t) = \hat{v}(0), \quad t > 0, \quad (2.23)$$

because $\text{Re}(\lambda_1) \leq 0$. However, putting $\lambda_1 = \lambda_2 = 0$ yields the unbounded linearly growing solution mode

$$\hat{u}(t) = \hat{u}_0 + t\hat{v}_0, \quad \hat{v}(t) = \hat{v}_0, \quad t > 0, \quad (2.24)$$

which opposes stability in the sense of bounded solutions for all $t \geq 0$. Here model (2.20) reveals why A_2 is required to be symmetric negative definite for having all possible solutions bounded.

Any consistent Runge-Kutta method will compute solution (2.24) exactly. However, the true linear growth for $\lambda_1 = \lambda_2 = 0$ will be accompanied with a similar linear growth of round-off and (possibly) truncation errors which cannot be avoided. Unbounded linear error growth cannot occur if $\text{Re}(\lambda_1) < 0$ or $\lambda_2 < 0$, but for small eigenvalues significant growth can still manifest itself over long time intervals which can also be interpreted as bad conditioning. We will explain and discuss this numerical issue in Section 3.3.

Ansatz 2.5 *Matrix A is similar to a diagonal eigenvalue matrix with eigenvalues λ satisfying $\text{Re}(\lambda) \leq 0$ and its set of eigenvectors does have a condition number independent of m .* \diamond

This Ansatz serves to cover cases where A_1 and A_2 do not commute so that model (2.20) is not applicable. Write $A = X\Lambda X^{-1}$. For the solution $w(t)$ of problem (2.4) with a zero source term we then have in any norm

$$\|w(t)\| \leq \text{cond}(X) \|w(0)\| \|e^{\Lambda t}\|, \quad t \geq 0, \quad (2.25)$$

hence a bounded (stable) solution for all $t \geq 0$. Ansatz (2.5) covers in fact the standard assumption made in linear stability analysis of numerical methods for ODEs and, similar to Ansatz (2.4), will enable us to use the stability region concept.

For this Ansatz the similarity transformation (2.16) based on a symmetric negative definite matrix A_2 is also relevant. If (2.16) applies matrix A has the same eigenvalues as the transformed matrix \tilde{A} and from the symmetric part

$$\begin{pmatrix} \frac{1}{2}(A_1 + A_1^T) & 0 \\ 0 & 0 \end{pmatrix} \quad (2.26)$$

of \tilde{A} follows that if the spectral abscissa or the logarithmic norm $\mu_2(A_1)$ is bounded by some constant ω , there holds

$$\|w(t)\|_2 \leq C \|w(0)\|_2 e^{\omega t}, \quad t \geq 0, \quad (2.27)$$

where C is the L_2 -condition number of the transforming matrix in (2.16), see [14], Sect. I.2.3. So we can conclude stability in the L_2 -norm if $\omega \leq 0$.

2.3 Illustration

Before turning our attention to the Runge-Kutta methods we will illustrate the above for the one-space dimensional problem

$$\begin{aligned} U_{tt} &= (\mathcal{L}_1 U)_t + \mathcal{L}_2 U, \\ \mathcal{L}_1 U &= \gamma_1 U - (a(x)U)_x + (d_1(x)U_x)_x, \quad t > 0, \quad 0 \leq x \leq 1, \\ \mathcal{L}_2 U &= \gamma_2 U + (d_2(x)U_x)_x, \end{aligned} \quad (2.28)$$

assuming 2nd-order symmetrical differencing on a uniform space grid of width $h = 1/m$,

$$\begin{aligned} (a(x)U)_x &\approx \frac{a_+ U(x+h) + (a_+ - a_-) U(x) - a_- U(x-h)}{2h}, \\ (d(x)U_x)_x &\approx \frac{d_+ U(x+h) - (d_+ + d_-) U(x) + d_- U(x-h)}{h^2}. \end{aligned} \quad (2.29)$$

Here $a_{\pm} = a(x \pm h/2)$, $d_{\pm} = d(x \pm h/2)$ and $d(x)$ represents $d_1(x) \geq 0$ or $d_2(x) \geq 0$. Further, we assume $\gamma_1(x) \leq 0$ and $\gamma_2(x) \leq 0$ and periodicity in space. For the resulting semi-discrete system (2.4) we will first illustrate the Ansatzes we made and then we will show two typical solutions.

Regarding Ansatz (2.1) and (2.2) we consider the standard L_2 -inner product and norm

$$\langle u, \tilde{u} \rangle_2 = h \sum_{j=1}^m u_j \tilde{u}_j, \quad \|u\|_2^2 = \langle u, u \rangle_2, \quad (2.30)$$

which can be used since we semi-discretize in the conservative form. For this inner product our matrix A_2 is immediately seen to be symmetric, non-positive definite complying with Ansatz 2.1. Due to periodicity A_2 can have a zero eigenvalue associated with spatially constant solutions. If we take γ_2 strictly negative matrix A_2 becomes symmetric negative definite complying with Ansatz 2.2. Next consider matrix A_1 which we write as $A_1 = A_{1a} + A_{1d}$ where A_{1a} represents the advection matrix and A_{1d} the diffusion matrix including the scalar function $\gamma_1(x)$. Similar as for A_2 it follows immediately that A_{1d} is symmetric, non-positive definite. For A_{1a} holds (see [14], Sect. I.4.3)

$$\langle A_{1a} u, u \rangle_2 \leq \frac{1}{2} \omega_1 \|u\|_2^2, \quad \omega_1 = \frac{1}{h} \max_j \left(a(x_{j-\frac{1}{2}}) - a(x_{j+\frac{1}{2}}) \right), \quad (2.31)$$

and $\omega_1 = \mathcal{O}(1)$ uniformly in h if $a(x)$ is assumed to be differentiable. Since A_{1d} is symmetric, non-positive definite this so-called one-sided Lipschitz condition also holds for matrix A_1 with the same ω_1 in compliance with Ansatz 2.2. The condition on A_1 of Ansatz 2.1 will hold only for special coefficient choices.

Considering Ansatz 2.4, let us next assume constant coefficients a, d_1, d_2 and let us take $\gamma_1(x)$ and $\gamma_2(x)$ equal to zero, just for convenience. Then, applying Fourier-von Neumann analysis, Ansatz 2.4 holds with the eigenvalues

$$\begin{aligned}\lambda_1 &= -\frac{ia}{h} \sin(2\pi kh) - \frac{4d_1}{h^2} \sin^2(\pi kh), \\ \lambda_2 &= -\frac{4d_2}{h^2} \sin^2(\pi kh),\end{aligned}\quad k = 1, \dots, m. \quad (2.32)$$

Based on these eigenvalues, Figure 2.1 shows typical spectra for λ_{\pm} defined in (2.22) for $(a, d_1, d_2) = (0, 0, 1)$ (left plot), $(0, 1, 1)$ (second left), $(1, 1, 1)$ (second right), $(1, 0, 1)$ (right). The first choice is for the model acoustic wave equation for which we have a purely imaginary spectrum, the second includes damping resulting in an extended real non-positive spectrum, the third includes damping as well as advection giving rise to complex eigenvalues, and the fourth includes advection only resulting in a purely imaginary spectrum.

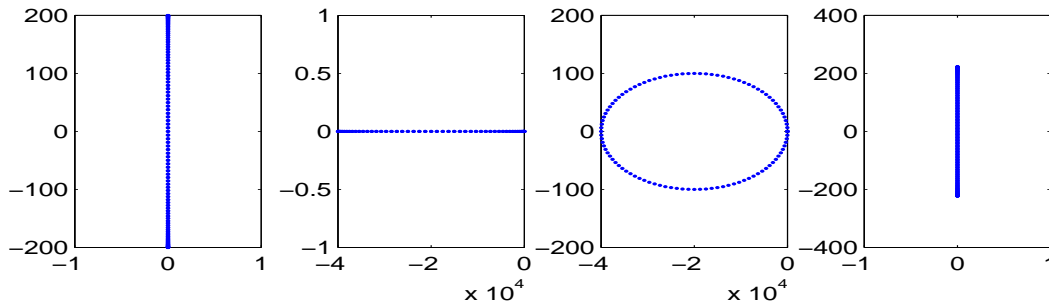


Figure 2.1: Eigenvalue spectra λ_{\pm} based on (2.32). Here $m = 100$.

Ansatz 2.5 comes into play if our matrices A_1 and A_2 do not commute which normally holds for variable coefficients. If γ_2 is strictly negative A_2 is symmetric negative definite so that inequality (2.27) applies. Whether then $\omega \leq 0$ will depend on the advection coefficient $a(x)$. However, following the reasoning above behind the one-sided Lipschitz condition (2.31), we do know that $\omega = \mathcal{O}(1)$ and thus is independent of m . In this sense the problem is well conditioned.

Finally, in Figure 2.2 we show two typical non-viscous wave forms for $0 \leq t \leq 3$ defined by the initial values $U(x, 0) = \cos(\pi(x - \frac{1}{2}))^{100}$, $U_t(x, 0) = 0$ and the constant coefficients $(a, d_1, d_2) = (0, 0, 1), (1, 0, 1)$, whereby again the γ -values are taken zero. The first coefficient choice gives the undamped exact solution

$$U(x, t) = (U(x + t, 0) + U(x - t, 0))/2, \quad (2.33)$$

and the second implies advection on top of it. The advection term can be seen to change the speed and profile of the wave form significantly. We have plotted approximate solutions obtained by accurate numerical integration using the spatial discretization (2.29) for $h = 1/200$. Adding viscosity can be done in many ways and will necessarily smooth these profiles.

3 Runge-Kutta methods

For the ODE system (2.2) the general form of a Runge-Kutta method is

$$\begin{aligned}w_{n+1} &= w_n + \tau \sum_{i=1}^s b_i F(t_n + c_i \tau, w_{ni}), \\ w_{ni} &= w_n + \tau \sum_{j=1}^s \alpha_{ij} F(t_n + c_j \tau, w_{nj}), \quad i = 1, \dots, s.\end{aligned}\quad (3.1)$$

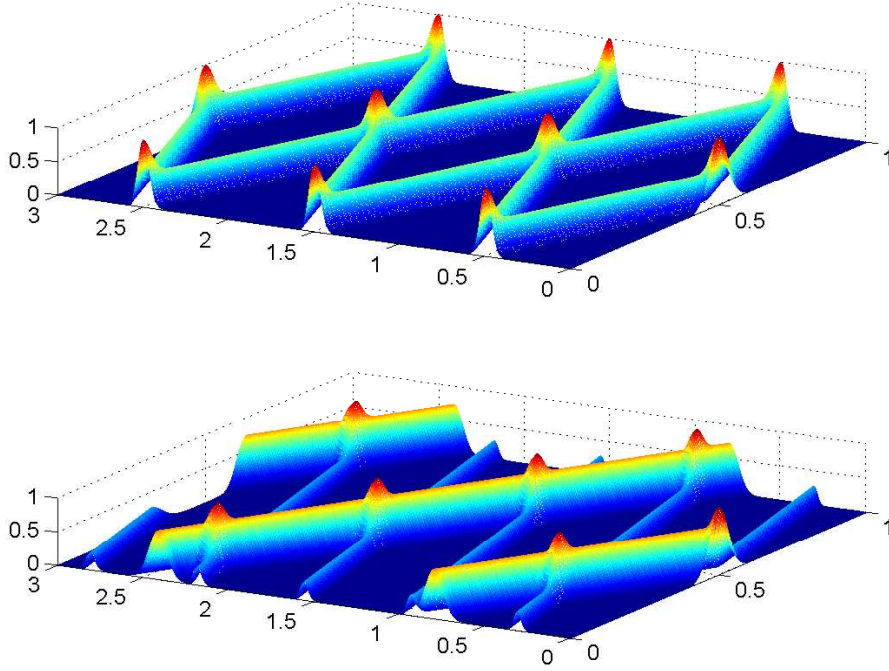


Figure 2.2: Two numerical solutions for $U(x, t)$, $0 \leq x \leq 1$, $0 \leq t \leq 3$ of problem (2.28). On top solution (2.33) and below advection added to it, both with clipping of negative values.

Here w_n and w_{n+1} denote approximations to $w(t_n)$ and $w(t_{n+1})$. With this method we thus advance in time from t_n to $t_{n+1} = t_n + \tau$ using the step size τ which may vary. The w_{ni} are intermediate (stage) approximations to $w(t_n + c_i\tau)$, α_{ij} and b_i are the coefficients defining the particular Runge-Kutta method and s denotes the number of stages. Throughout we adopt the convention $c_i = \sum_{j=1}^s \alpha_{ij}$.

The theory and implementation of Runge-Kutta methods for ODEs is extensive and mature which has led to efficient explicit ($\alpha_{ij} = 0$, $j \geq i$), diagonally implicit ($\alpha_{ij} = 0$, $j > i$) and fully implicit methods and software [5, 8, 12, 13, 20, 22]. For truly large-scale problems as we have with semi-discrete PDEs in multiple space-dimension, the implicit methods meet restrictions as they require the solution of large systems of algebraic equations. This is most severe for the fully implicit methods because then the s intermediate approximations w_{ni} are coupled. For diagonally implicit methods solving is easier as we then can solve for $w_{n1}, w_{n2}, \dots, w_{ns}$ in a subsequent manner. On the other hand, explicit methods always meet step size restrictions for stability. If these step size restrictions are too severe the use of an unconditionally stable implicit method can still be a more attractive option.

Considering the viscous wave equation (2.3), in that case we favor the singly-implicit diagonally implicit methods having a_{ii} equal, say $a_{ii} = \gamma$. At each stage we then have to solve a 2×2 -block linear system of algebraic equations of the form

$$\begin{pmatrix} I - \gamma\tau A_1 & -\gamma\tau I \\ -\gamma\tau A_2 & 0 \end{pmatrix} \begin{pmatrix} u_{ni} \\ v_{ni} \end{pmatrix} = \begin{pmatrix} a \\ b \end{pmatrix}. \quad (3.2)$$

By using the Schur complement we can simplify this system such that we only need to solve for the u_{ni} and can obtain the v_{ni} explicitly,

$$\begin{aligned} (I - \gamma\tau A_1 - \gamma^2\tau^2 A_2) u_{ni} &= a + \gamma\tau b, \\ v_{ni} &= b + \gamma\tau A_2 u_{ni}. \end{aligned} \quad (3.3)$$

This is attractive when using a direct solver and τ is constant so that just a single decomposition

of $I - \gamma\tau A_1 - \gamma^2\tau^2 A_2$ is required.

The simplification from (3.2) to (3.3) holds generally for the ODE system (2.1) because the equation of (3.1) defining the u_{ni} can always be written as

$$u_{ni} = u_n + \tau c_i v_n + \tau \sum_{j=1}^s \alpha_{ij} F_1(t_n + c_j\tau, u_{nj}) + \tau^2 \sum_{j=1}^s \eta_{ij} F_2(t_n + c_j\tau, u_{nj}), \quad (3.4)$$

where $\eta_{ij} = \sum_{k=1}^s \alpha_{ik} \alpha_{kj}$. Having solved for the u_{ni} , the v_{ni} are then found by explicit substitution from

$$v_{ni} = v_n + \tau \sum_{j=1}^s \alpha_{ij} F_2(t_n + c_j\tau, u_{nj}). \quad (3.5)$$

Because F_2 and likewise A_2 are stiff, the u_{ni} are to be solved in sufficiently high accuracy. If not, explicit substitution can amplify small but stiff perturbations which will hinder the integration. If $d = 1$ in (1.1), solving for the u_{ni} with a band solver should render no serious computational problem. If $d = 2$ a sparse matrix solver is certainly advocated, while if $d = 3$ one readily has to resort to an iterative linear solver. Such solvers are most efficient if both F_1 and F_2 are discrete symmetric elliptic operators which is true for the non-viscous wave equation problem ($A_1 = 0$) and for the viscous problem without advection terms.

3.1 Algebraic stability

This algebraic criterion was found independently by [2, 6] for proving the nonlinear stability property of B -stability due to [4]. Method (3.1) is called algebraically stable if $b_i \geq 0$ for $i = 1, \dots, s$ and the $s \times s$ symmetric matrix (m_{ij}) with entries $m_{ij} = b_i \alpha_{ij} + b_j \alpha_{ji} - b_i b_j$ is non-negative definite. We can use this criterion directly for proving the discrete counterparts of the stability results (2.10) and (2.15) with a zero constant ω_1 for algebraically stable implicit Runge-Kutta methods, that is, unconditional stability in the respective norms.

All what we need is the fundamental relation

$$\|w_{n+1}\|^2 = \|w_n\|^2 + 2\tau \sum_{i=1}^s b_i \langle Aw_{ni}, w_{ni} \rangle - \tau^2 \sum_{i,j=1}^s m_{ij} \langle Aw_{ni}, Aw_{nj} \rangle, \quad (3.6)$$

which holds for any Runge-Kutta method (3.1) applied to the ODE system (2.4) with zero source terms and any inner product $\langle \cdot, \cdot \rangle$, see the original papers [2, 6] or the monograph [8], Sect. 4.2 or [13], Sect. IV.12. The third term at the right-hand side is non-positive if matrix (m_{ij}) is non-negative definite and so is the second term if $\langle Aw_{ni}, w_{ni} \rangle \leq 0$ and the coefficients b_i are nonnegative. So then the stability inequality $\|w_{n+1}\| \leq \|w_n\|$ for all $\tau > 0$ follows while if $\langle Aw_{ni}, w_{ni} \rangle = 0$ and matrix (m_{ij}) is zero we immediately conclude the conservation property.

Among the classical implicit Runge-Kutta methods, the methods known under the names Gauss, Radau IA, Radau IIA and Lobatto IIIC are algebraically stable. There also exist diagonally implicit and so-called singly-implicit algebraically stable methods, see the aforementioned literature. The Gauss methods are special since they have a zero matrix (m_{ij}) and hence respect the conservation property $\langle Aw_{ni}, w_{ni} \rangle = 0$.

Example 3.1 As a concrete example let us consider the 2nd-order implicit midpoint rule. When formulated as a Runge-Kutta method (3.1) we have the 1-stage Gauss method

$$\begin{aligned} w_{n+1} &= w_n + \tau F(t_{n+1/2}, w_{n1}), \\ w_{n1} &= w_n + \frac{1}{2}\tau F(t_{n+1/2}, w_{n1}), \end{aligned} \quad (3.7)$$

for which relation (3.6) is immediately verified. Note that for the homogeneous part of the ODE system (2.4) this method is identical to the 2nd-order trapezoidal rule

$$w_{n+1} = w_n + \frac{1}{2}\tau A(w_n + w_{n+1}) + \frac{1}{2}\tau(s(t_n) + s(t_{n+1})), \quad (3.8)$$

which in the PDE literature is often called the Crank-Nicolson method. \diamond

Example 3.2 The implicit midpoint rule is a one-stage DIRK (Diagonally Implicit Runge-Kutta) method. Algebraic stability restricts the order of such methods to four [11]. An example of an algebraically stable 4th-order DIRK method due to [3] is defined by the Butcher array

$$\begin{array}{c|ccc} \gamma & \gamma & 0 & 0 \\ \frac{1}{2} & \frac{1}{2} - \gamma & \gamma & 0 \\ 1 - \gamma & 2\gamma & 1 - 4\gamma & \gamma \\ \hline & b & 1 - 2b & b \end{array} \quad \text{where} \quad \begin{aligned} \gamma &= \frac{1}{2} + \frac{1}{3}\sqrt{3}\cos\left(\frac{\pi}{18}\right), \\ b &= 1/(24(\frac{1}{2} - \gamma)^2). \end{aligned} \quad (3.9)$$

This method has three subsequent implicit stages compared to just one for implicit midpoint. Hence for large problems the costs are also about three times larger. Yet higher order can pay off when high temporal accuracy is required, for example in long time integration. Note that the algebraic stability matrix $(m_{ij}) \neq 0$ so that this method cannot mimic conservation. \diamond

3.2 A-stability

Many useful implicit Runge-Kutta methods (3.1) exist which are not algebraically stable but A -stable and variants thereof such as $A(\alpha)$ -stability and L -stability [5, 8, 12, 13, 20, 22]. Algebraic stability implies A -stability which for stiff ODEs is the most well-known numerical stability property. The notion of A -stability is due to Dahlquist [7] and is defined for his celebrated scalar test model $w' = \lambda w, \lambda \in \mathbb{C}$. Any p -th order consistent Runge-Kutta method (3.1) applied to $w' = \lambda w$ gives the scalar recurrence

$$w_{n+1} = R(z)w_n, \quad R(z) = e^z + \mathcal{O}(z^{p+1}), \quad z \rightarrow 0, \quad (3.10)$$

where $z = \tau\lambda$ and $R(z) = P(z)/Q(z)$ is the rational or polynomial stability function defined by (3.1). A -stability then is the property $|R(z)| \leq 1$ for all $z \in \mathbb{C}$ with $\text{Re}(z) \leq 0$ and thus implies $|w_{n+1}| \leq |w_n|$ for all $\tau > 0$ and all $\lambda \in \mathbb{C}$ such that $\text{Re}(\lambda) \leq 0$.

For our model system (2.4) with a zero source term we have the related matrix recurrence

$$w_{n+1} = R(\tau A)w_n, \quad (3.11)$$

for which again the discrete counterparts of the stability properties (2.10) and (2.15) can be proven if the Runge-Kutta method is A -stable (hence algebraic stability is not necessary). All what we need for A -stable methods is the following theorem which originates from von Neumann [17]: let $\|\cdot\|$ be an inner product norm and suppose $\langle Aw, w \rangle \leq 0$, then $\|R(\tau A)\| \leq 1$ for all $\tau > 0$ for an A -stable stability function $R(z)$. See [13], Sect. IV.11 and [8], Sect. 2.3 for details on von Neumann's theorem and further references.

Example 3.3 An example of an A -stable (but not algebraically stable) 3rd-order DIRK method attributed to R. Alt, 1973 (see [14], Sect.II.1.2) is defined by the Butcher array

$$\begin{array}{c|ccc} 0 & 0 & 0 & 0 \\ 2\gamma & \gamma & \gamma & 0 \\ 1 & b_1 & b_2 & \gamma \\ \hline & b_1 & b_2 & \gamma \end{array} \quad \text{where} \quad \begin{aligned} \gamma &= \frac{1}{2} + \frac{1}{6}\sqrt{3}, \\ b_1 &= \frac{3}{2} - \gamma - \frac{1}{4\gamma}, \quad b_2 = -\frac{1}{2} + \frac{1}{4\gamma}. \end{aligned} \quad (3.12)$$

This method has two subsequent implicit stages of which the first is a trapezoidal rule step. Consequently, this method has stage order two since the order of the second implicit stage equals three due to the fact that $w_{n3} = w_{n+1}$. The stage order is the minimum of the consistency orders of the internal stages w_{ni} . Note that the stage order of the 4th-order method (3.9) equals one. A low stage order can be a disadvantage in connection with order reduction. We discuss this issue further in Section 3.4 \diamond

3.3 Stability regions

Ansatz 2.5 leads us to the familiar notion of stability region. Replace the exponential function in inequality (2.25) by the stability function giving

$$\|w_n\| \leq \text{cond}(X) \|w(0)\| \|R(\tau\Lambda)^n\|, \quad n \geq 0. \quad (3.13)$$

We have stability in the sense of w_n bounded for all $n \geq 0$ if $|R(z)| \leq 1$ for all entries $z = \tau\lambda$ of $\tau\Lambda$. The domain in \mathcal{C} for which $|R(z)| \leq 1$ is called the stability region or stability domain. The domain of A -stable implicit methods includes the whole of the left half of the complex plane, whereas for explicit methods domains are finite.

Figure 3.1 illustrates this for the Padé polynomial $R(z) = \sum_{j=0}^4 z^j/j!$ being the stability polynomial of the classical, 4th-order explicit Runge-Kutta method and for the modified polynomial

$$R(z) = \sum_{j=0}^4 \frac{z^j}{j!} + \frac{z^5}{240}. \quad (3.14)$$

This 5th-degree polynomial was obtained in [15] in connection with optimal monotonicity properties of polynomials approximating the exponential function. We mention it here as it shows that with one additional function evaluation the real stability interval is doubled from 2.78 to 5.89, approximately. Hence, compared to the standard Padé polynomial, the modified polynomial might be of interest if the viscous part of (1.1) is sufficiently small for an explicit treatment provided one also wishes to treat the non-viscous part explicitly. For the standard Padé polynomial the imaginary stability interval is known to have length $2\sqrt{2}$, while for the modified polynomial this length amounts to 3.20, approximately. Hence for imaginary eigenvalues nothing is gained because the length scaled by the number of function evaluations decreases from 0.70 to 0.64, approximately. In [15] no explicit Runge-Kutta method is given having (3.14) as stability polynomial, but such a method can be constructed.

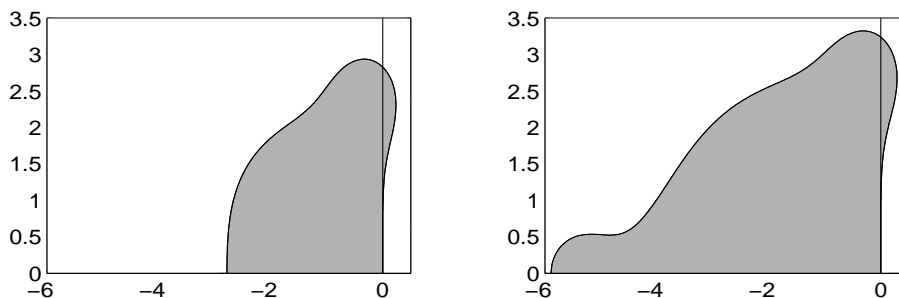


Figure 3.1: Stability regions for the 4th-order Padé polynomial (left) and the modified 4th-order Padé polynomial (3.14) (right).

We next assume Ansatz 2.4 which enables us to use the 2×2 test model (2.20), simply by again replacing the exponential function by the stability function. This yields the recurrence

$$\begin{pmatrix} \hat{u}_{n+1} \\ \hat{v}_{n+1} \end{pmatrix} = R \begin{pmatrix} \tau\lambda_1 & \tau \\ \tau\lambda_2 & 0 \end{pmatrix} \begin{pmatrix} \hat{u}_n \\ \hat{v}_n \end{pmatrix}, \quad (3.15)$$

which we rewrite to

$$\begin{pmatrix} \hat{u}_{n+1} \\ \tau\hat{v}_{n+1} \end{pmatrix} = R \begin{pmatrix} z_1 & 1 \\ -z_2^2 & 0 \end{pmatrix} \begin{pmatrix} \hat{u}_n \\ \tau\hat{v}_n \end{pmatrix}, \quad z_1 = \tau\lambda_1, \quad z_2 = \tau\sqrt{-\lambda_2}. \quad (3.16)$$

If $\lambda_2 \neq 0$ the 2×2 matrix can be diagonalized, which shows that for stability it is necessary that its eigenvalues

$$z_{\pm} = \frac{1}{2} \left(z_1 \pm \sqrt{z_1^2 - 4z_2^2} \right) \quad (3.17)$$

lie in the stability domain, cf. (2.22).

This, however, is not sufficient. An additional necessary condition is that $z_- \neq z_+$ if $|R(z_-)| = |R(z_+)| = 1$ (the root condition). This condition is violated for $\lambda_1 = \lambda_2 = 0$. If $\lambda_2 = 0, \lambda_1 \neq 0$ recurrence (3.16) is replaced by

$$\begin{pmatrix} \hat{u}_n \\ \tau \hat{v}_n \end{pmatrix} = \begin{pmatrix} R^n(z_1) & \frac{R(z_1)-1}{z_1} \sum_{j=0}^{n-1} R^j(z_1) \\ 0 & 1 \end{pmatrix} \begin{pmatrix} \hat{u}_0 \\ \tau \hat{v}_0 \end{pmatrix}. \quad (3.18)$$

Consistency implies $R(0) = 1$, so that also putting $\lambda_1 = 0$ gives

$$\begin{pmatrix} \hat{u}_n \\ \tau \hat{v}_n \end{pmatrix} = \begin{pmatrix} 1 & n \\ 0 & 1 \end{pmatrix} \begin{pmatrix} \hat{u}_0 \\ \tau \hat{v}_0 \end{pmatrix}, \quad (3.19)$$

which returns the exact linear solution (2.24). Hence for $\lambda_1 = 0, \lambda_2 = 0$ we face unbounded linear growth. This linear growth is of course not an artefact of the method. It is an inherent problem property and a numerical integration method not showing this growth cannot be consistent. However, it does imply linear growth of round-off (and possibly truncation errors), while for solution modes with eigenvalues close to zero also growth will occur as exemplified by the (2, 2)-entry of (3.18). Such growth is of course bounded if $|R(z_1)| < 1$ but it can manifest itself over long time intervals if $R(z_1)$ is very close to one. Example 3.4 below illustrates this.

Example 3.4 Although simple, the driven damped oscillator problem

$$\begin{pmatrix} \hat{u}' \\ \hat{v}' \end{pmatrix} = \begin{pmatrix} \lambda_1 & 1 \\ \lambda_2 & 0 \end{pmatrix} \begin{pmatrix} \hat{u} \\ \hat{v} \end{pmatrix} + \begin{pmatrix} 0 \\ \hat{s}(t) \end{pmatrix} \quad (3.20)$$

derived from $\hat{u}'' - \lambda_1 \hat{u}' - \lambda_2 \hat{u} = \hat{s}(t)$ serves our purpose. We choose the transient steady-state solution $\hat{u}(t) = \sin(2\pi t)$ and adjust $\hat{v}(t)$ and forcing $\hat{s}(t)$ accordingly. We have integrated with the 4th-order DIRK method (3.9) using $\tau = 0.1$ over the long time interval $[0, 10^4]$ for the (λ_1, λ_2) -values

$$(\lambda_1, \lambda_2) = \begin{cases} (0, 0) & (0, -10^{-3}) & (0, -10^{-2}) \\ (-10^{-3}, 0) & (-10^{-3}, -10^{-3}) & (-10^{-2}, -10^{-2}) \end{cases} \quad (3.21)$$

So in the first row $\lambda_1 = 0$ (no damping) and in the second $\lambda_1 = \lambda_2$ except in the first entry where $\lambda_2 = 0$. For these six cases Figure 3.2 shows the error evolution in u plotted at times $t_j = 10^2 j, j = 1, 2, \dots, 10^2$. Noting the scaling of the vertical axes we observe the anticipated differences in the error, in particular the growth of the truncation error in the upper plots for $\lambda_2 = 0$, being linear in the left plot and bounded and pertaining in the right one.

As mentioned before, this growth cannot be avoided. The only remedy is to integrate with a higher order method resulting in smaller truncation errors. On the other hand, the current problem is artificial in the sense that we do have a truncation error for $\lambda_1 = \lambda_2 = 0$ by our special choice of source term. We also encounter this singularity in problem (2.28) due to periodicity resulting in constant-in-space – linear-in-time solution modes. These modes are solved exactly by any consistent numerical method leaving us only with linear round-off error growth. \diamond

3.4 Stiff source terms

Runge-Kutta methods have very good stability properties and there exists no limit on their consistency order. However, for stiff source terms $s(t)$ in (2.4), and thus for PDEs (1.1) with time-dependent boundary conditions, they show a deficiency called order reduction which can be a disadvantage in high accuracy calculations. It occurs on fine enough fixed space grids or if simultaneously the temporal and spatial grid is refined. Order reduction is a property of the integration method, not of the spatial discretization. If simultaneously the temporal and spatial grid is refined,

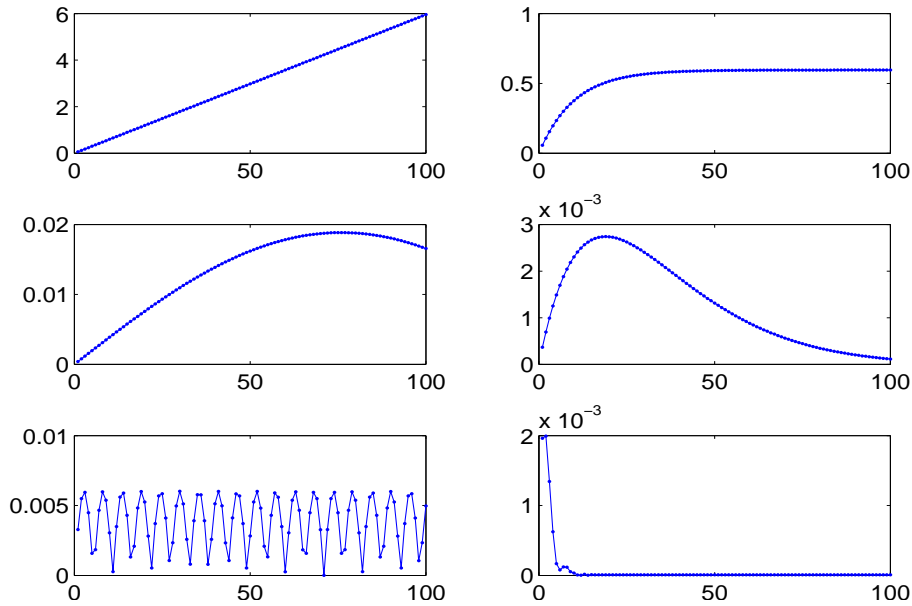


Figure 3.2: The driven oscillator test. Vertical axis: absolute errors in u . Horizontal axis: $t/100$. Left column for the first row of values (3.21), right column for the second row. The two upper plots represent the first pair in the two rows, etc.

in terms of temporal order of convergence it implies a global order to the PDE solution generally equal to $\min(p, q)$ instead of p , where p denotes the order of ODE consistency and $q \leq p$ the related stage order. One also encounters the order $\min(p, q + 1)$ due to cancellation of local errors. Such cancellation is method and problem dependent. If only the temporal grid is refined and the space grid is fixed, in the limit the ODE order p applies. But on fine grids the observed computational order can be much closer to $\min(p, q)$ or $\min(p + 1, q)$ or one may encounter uncommonly large error constants determined by the spatial grid size. Order reduction for PDEs is nowadays well understood, see e.g. [14], Sect. II.2.1 and references therein, and is intimately related to order reduction for stiff ODEs, see [8], Ch.7 and [13], Sect. IV.15. Regarding PDEs, order reduction does not occur with periodic boundary conditions.

Various techniques have been proposed to repair the order. An easily applicable one was recently proposed in [19]. This technique is akin to a technique from [1] and amounts to correcting the source term $s(t)$ of (2.4) as follows, componentwise described. Let $g(t)$ be a component of $s(t)$. Let $\mathbf{A} = (a_{ij})$ be the $s \times s$ matrix of coefficients a_{ij} of the Runge-Kutta method (3.1), let $\mathbf{g}(t) = [g(t + c_1\tau), \dots, g(t + c_s\tau)]^T$ and $\mathbf{e} = [1, \dots, 1]^T$. The source component $g(t)$ is then corrected over the Runge-Kutta stages to

$$\mathbf{g}_m(t) = \mathbf{e}g(t) + \mathbf{A}\tau\ddot{\mathbf{g}}(t) \quad \text{or} \quad \mathbf{g}_m(t) = \mathbf{e}g(t) + \mathbf{A}\mathbf{e}\tau\dot{g}(t) + \mathbf{A}^2\tau^2\ddot{\mathbf{g}}(t), \quad (3.22)$$

replacing $g(t + c_i\tau)$ by the i -th component of $\mathbf{g}_m(t)$ for $i = 1, \dots, s$. The left formula increases the stage order by one unit which for the 3rd-order DIRK method (3.12) having $p = 3, q = 2$ is just enough to recover its ODE order for stiff source terms. Likewise, the right formula increases the stage order q by two units which for the 4th-order DIRK method (3.9) having $p = 4, q = 1$ is just enough to recover its ODE order for stiff source terms, assuming local error cancellation adds another unit of convergence. The formulas (3.22) taken from [19] have been designed such that they do not affect the order for non-stiff source terms. They were derived for Rosenbrock methods applied to linear problems of type (2.4) and also work for DIRK methods.

Example 3.5 To illustrate the order reduction and the correction formulas (3.22) we have solved

$$U_{tt} = (U_{xx})_t + U_{xx} + s(x, t), \quad t > 0, \quad 0 < x < 1, \quad (3.23)$$

for the exact solution $U(x, t) = x^2 \sin(t)$ and Dirichlet boundary conditions so that the solution at the boundary $x = 1$ is time dependent. In spite of its simplicity, this simple setting serves our purpose. The third-order method (3.12) was applied with and without the left correction formula (3.22) and the fourth-order method (3.9) with and without the right one, always over the time interval $[0, T]$, $T = \pi/2$. A uniform space grid of width h was used with 2nd-order central differences giving a zero space error due to the quadratic dependence. We have solved the problem for $h = 1/(m + 1)$, $\tau = T/m$ and $h = 1/321$, $\tau = T/m$ for $m = 5, 10, \dots, 320$. These two space-time grids gave nearly the same results. Figure 3.3 shows the results for the simultaneous space-time refinement. The 3rd-order method benefits from local cancellation, so that also without correction the ODE order $p = 3$ is recovered while the accuracies are nearly the same. Also the 4th-order one benefits from local cancellation, resulting in order $q = 2$ without correction and order $p = 4$ with correction. Clearly, the 4th-order method truly benefits from the correction. This will also be true for the 3rd-order method in cases without the benefit of local error cancellation. \diamond

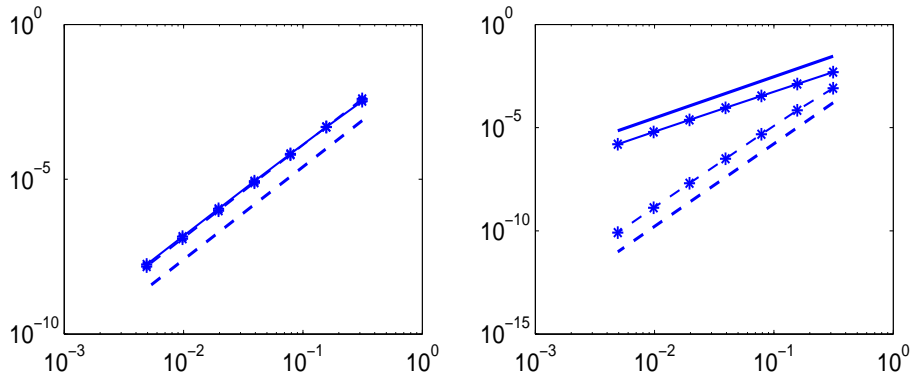


Figure 3.3: The order reduction experiment for problem (3.23). Log-log plots showing the maximum global error at the end time T along the vertical and the step size τ along the horizontal axes. At the left the 3rd-order method (3.12), at the right the 4th-order method (3.9). Dashed lines represent cases with correction, lines with markers observed orders and lines without markers theoretical orders.

4 A stiff test example

An immediate consequence of adding viscous terms is stiffness. The following two-space dimensional problem subjected to periodic boundary conditions provides another stiff example:

$$U_{tt} = ((d(\pi x)U_x)_x + (d(\pi y)U_y)_y)_t + U_{xx} + U_{yy}, \quad (4.1)$$

where $t > 0$, $0 \leq x, y \leq 1$ and $d(z) = \cos(z)^{100}$. The diffusion coefficients $d(\pi x)$ and $d(\pi y)$ are equal to one on the vertical and horizontal boundary, respectively, and rapidly decay to zero inward the unit square. For matrix A obtained on a uniform 50×50 space grid with spatial discretization by the 2nd-order symmetric difference formula from (2.29) these diffusion coefficients lead to the rather special cross-shaped spectrum shown in Figure 4.1. Most of the eigenvalues reside near the imaginary axis while a few of them are real large negative causing A to be stiff as if we were dealing with a diffusion equation.

For illustrating a typical solution to (4.1) we impose the initial values

$$U(x, y, 0) = d(\pi(x + y - 1)), \quad U_t(x, y, 0) = 0 \quad (4.2)$$

at time $t = 0$. Without the viscous term we then have

$$U(x, y, t) = \frac{1}{2}d(\pi(x + y - 1 + \sqrt{2}t)) + \frac{1}{2}d(\pi(x + y - 1 - \sqrt{2}t)) \quad (4.3)$$

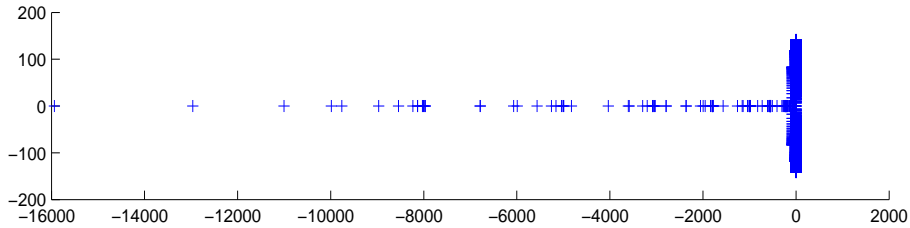


Figure 4.1: The eigenvalues of a semi-discretization of problem (4.1).

as exact solution. The choice of diffusion coefficients locally implies that before the wave reaches the boundary its profile remains unchanged while at later times it is smoothed over the entire space domain. Figure 4.2 illustrates this with the non-viscous exact solution (4.3) plotted for $0 \leq t \leq 1$ along the line $0 \leq x \leq 1, y = 0.5$ (upper plot) and along the same line and time interval an approximation to the viscous solution (lower plot with clipping of negative values). This approximation was obtained by accurate time integration on a uniform 200×200 space grid and with spatial discretization by the 2nd-order central formula used above.

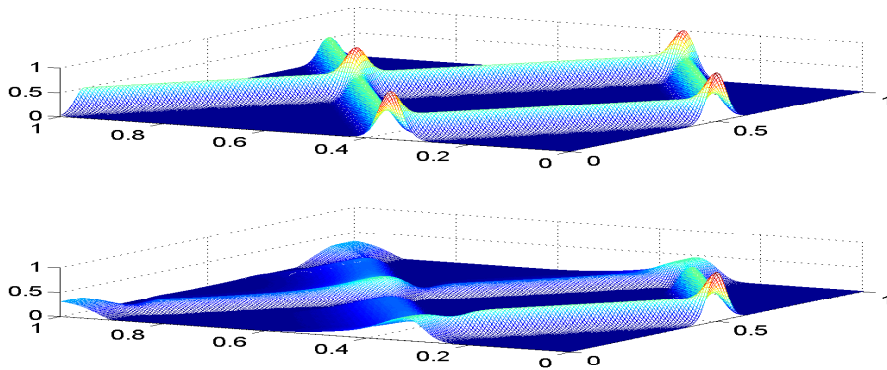


Figure 4.2: Solutions to problem (4.1) along the line $0 \leq x \leq 1, y = \frac{1}{2}$. Temporal direction front left.

Substantial stiffness rules out explicit integrators in use for non-viscous wave equations. Unconditionally stable implicit methods like those of Runge-Kutta type are then indispensable. We conclude the paper with presenting test results for the three A -stable DIRK methods mentioned in Section 3 applied to the viscous semi-discrete system obtained on the 100×100 space grid. The loglog plot given in Figure 4.3 shows efficiency, that is, we plot maximum norm ODE errors taken along the grid line $0 \leq x \leq 1, y = \frac{1}{2}$ at time $t = 1$ versus computational work. The errors are measured against a sufficiently accurate numerically computed reference solution. Work is expressed as number of time steps times number of effective stages, which is one for the 2nd-order method (3.7), two for the 3rd-order method (3.12) and three for the 4th-order method (3.9). For all three DIRK methods the marks in the plot refer to the step sizes $\tau = \frac{1}{50}2^{-k}, k = 0, \dots, 5$. The methods were implemented with the simplified linear system form (3.3) using LU-decomposition.

We deal here with an homogeneous linear system $w' = Aw$, which means that we actually measure errors of the stability matrix functions of the three methods against the exponential matrix function, that is, differences $(e^{An\tau} - R(\tau A)^n)w_0, n\tau = 1$. Because we take into account workload the advantage of using higher order methods is borne out only in the high accuracy region, as to be expected. For moderate temporal accuracy we see not much difference here, whereas for low accuracy the lower order method appears to be most efficient. Needless to say that all of this depends on the smoothness of the solution and that there is no doubt that with a more smooth solution or a higher-order space discretization higher-order time stepping will readily

become more advantageous.

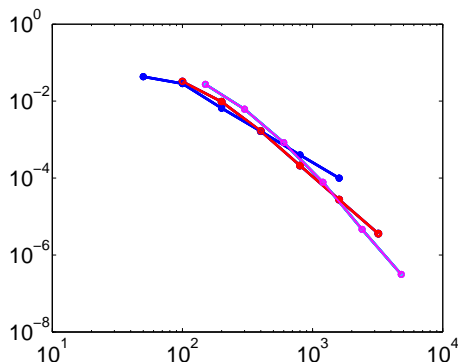


Figure 4.3: ODE convergence of the DIRK methods applied to the stiff viscous problem (4.1)-(4.2). Error and work along the vertical and horizontal axis, respectively. Second-order method blue color, third-order method red, fourth-order magenta.

References

- [1] I. Alonso-Mallo, B. Cano (2002), *Spectral/Rosenbrock discretizations without order reduction for linear parabolic problems*. Appl. Numer. Math. 41, pp. 247–268.
- [2] K. Burrage, J.C. Butcher (1979), *Stability criteria for implicit Runge-Kutta methods*. SIAM J. Numer. Anal. 16, pp. 46–57.
- [3] K. Burrage (1982), *Efficiently implementable algebraically stable Runge-Kutta methods*. SIAM J. Numer. Anal. 19, pp. 245–258.
- [4] J.C. Butcher (1975), *A stability property of implicit Runge-Kutta methods*. BIT 15, pp. 358–361.
- [5] J.C. Butcher (1987), *The Numerical Analysis of Ordinary Differential Equations*. John Wiley & Sons, Chichester.
- [6] M. Crouzeix (1970), *Sur la B-stabilité des méthodes de Runge-Kutta*. Numer. Math. 32, pp. 75–82.
- [7] G. Dahlquist (1963), *A special stability problem for linear multistep methods*. BIT 3, pp. 27–43.
- [8] K. Dekker, J.G. Verwer (1984), *Stability of Runge-Kutta Methods for Stiff Nonlinear Differential Equations*. North-Holland, Amsterdam.
- [9] J. Douglas Jr., S. Lim, H. Lim (2003), *An improved alternating-direction method for a viscous wave equation*. Contemporary Mathematics 329, pp. 99–104.
- [10] G.H. Golub, C.F. van Loan (1996), *Matrix Computations*. Third edition, John Hopkins Univ. Press, Baltimore.
- [11] E. Hairer (1980), *Highest possible order of algebraically stable diagonally implicit Runge-Kutta methods*. BIT 20, pp. 254–256.
- [12] E. Hairer, S.P. Nørsett, G. Wanner (1993), *Solving Ordinary Differential Equations I – Nonstiff Problems*. Second edition, Springer Series in Computational Mathematics, Vol. 8, Springer-Verlag, Berlin.

- [13] E. Hairer, G. Wanner (1996), *Solving Ordinary Differential Equations II – Stiff and Differential-Algebraic Problems*. Second edition, Springer Series in Computational Mathematics, Vol. 14, Springer-Verlag, Berlin.
- [14] W. Hundsdorfer, J.G. Verwer (2003), *Numerical Solution of Time-Dependent Advection-Diffusion-Reaction Equations*. Springer Series in Computational Mathematics, Vol. 33, Springer, Berlin.
- [15] J.F.B.M. Kraaijevanger (1986), *Absolute monotonicity of polynomials occurring in the numerical solution of initial value problems*. Numer. Math. 48, pp. 303-322.
- [16] H. Lim, S. Kim, J. Douglas Jr. (2007), *Numerical methods for viscous and nonviscous wave equations*. Appl. Numer. Math. 57, pp. 194-212.
- [17] J. von Neumann (1951), *Eine Spektraltheorie für allgemeine Operatoren eines unitären Raumes*. Mathematischen Nachrichten 4, p. 258-281.
- [18] A. Prothero, A. Robinson (1974), *On the stability and accuracy of one-step methods for solving stiff systems of ordinary differential equations*. Math. Comp. 28, pp. 145-162.
- [19] V. Savcenco (2007), *Construction of high-order multirate Rosenbrock methods for stiff ODEs*. CWI report MAS-E0716, <http://ftp.cwi.nl/CWIreports/MAS/MAS-0716.pdf> (preprint).
- [20] L.F. Shampine (1994), *Numerical Solution of Ordinary Differential Equations*. Chapman & Hall, New York.
- [21] B.P. Sommeijer, J.G. Verwer (2007), *On stabilized integration for time-dependent PDEs*. J. Comput. Phys. 224, pp. 3-16.
- [22] H.J. Stetter (1973), *Analysis of Discretization Methods for Ordinary Differential Equations*. Springer-Verlag.